Available online at www.eccomasproceedia.org
Eccomas Proceedia COMPDYN (2023) 2204-2216

ECCOMAS
Proceedia

COMPDYN 2023
9th ECCOMAS Thematic Conference on
Computational Methods in Structural Dynamics and Earthquake Engineering
M. Papadrakakis, M. Fragiadakis (eds.)
Athens, Greece, 12-14 June 2023

VARIABLE ORIFICE DAMPER IMPLEMENTATION FOR SEISMIC SEMI-ACTIVE CONTROL OF CIVIL STRUCTURES

Andrea Troise[1], Eleonora Bruschi[2], Marco M. Rosso[1], Angelo Alosio[3], Alessandro Rizzo[1], Nikos D. Lagaros[4],Virginio Quaglini[2], and Giuseppe C. Marano[1]

[1] Politecnico di Torino, DISEG, Department of Structural, Geotechnical and Building Engineering
Corso Duca Degli Abruzzi, 24, Turin 10128, Italy
e-mail: {andrea.troise,marco.rosso, alessandro.rizzo, giuseppe.marano}@polito.it

[2] Politecnico di Milano, DABC, Department of Architecture, Built Environment and Construction Engineering
Piazza Leonardo da Vinci 32, Milan 20133, Italy
e-mail: {eleonora.bruschi, virginio.quaglini}@polimi.it

[3] Università degli Studi dell'Aquila, Civil Environmental and Architectural Engineering Department,
via Giovanni Gronchi n.18, L'Aquila 67100, Italy
e-mail: angelo.aloisio1@univaq.it

[4] National Technical University Athens, Institute of Structural Analysis & Seismic Research,
Zografou Campus, Athens 157 80, Greece
e-mail: nlagaros@central.ntua.gr

Abstract. *The existing strategies for improving the dynamic response of structures during seismic events can be categorized into passive, active, and semi-active control. Passive strategies provide a redesign of the structural dynamic parameters without employing any real-time control. Active control strategies are more effective than the previous one, but also more expensive. Furthermore, a relevant amount of energy supply is required during seismic events, which is a quite unrealistic scenario. Semi-active control strategies represent a compromise between the two previously mentioned strategies. These latters provide real-time control, less induced costs, and require less power supply. In this study, the behaviour and effectiveness of a semi-active damper have been analyzed. A single degree of freedom (DOF) system has been implemented in the Matlab Simulink environment equipped with a semi-active fluid viscous damper model. Two main control algorithms of the semi-active device have been considered: a proportional-integral-derivative (PID) and a model predictive control (MPC) controller. The control algorithms were designed by linearizing the device constitutive model and implementing their non-linearity through the characteristic equation of the device. Different levels of approximation of the model were considered, in conjunction with different sampling time rates to examine the delay effect of a possible practical implementation of the proposed system.*

Keywords: Variable orifice dampers, structural dynamics, semi-active control, proportional integral derivative controllers, model predictive control.

ISSN:2623-3347 © 2023 The Authors. Published by Eccomas Proceedia.
Peer-review under responsibility of the organizing committee of COMPDYN 2023.
doi: 10.7712/120123.10553.20285

1 INTRODUCTION

Structural control devices aim to mitigate the response of structural systems due to dynamic natural hazards, e.g. wind, earthquakes, etc. [6, 14]. During the last four decades, three main typologies of devices have been formalized, viz. active, passive, and semi-active devices [6, 21, 13]. In active damping energy devices, electrohydraulic or electromechanical actuators' control forces modify the dynamics of the structural response [22], with theoretical advantages of high performances, lower sensitivity to ground behavior, selectivity of the control strategy, and adaptability to various operating conditions [5]. The main drawback is the requirement for a consistent amount of external energy supply, which is a critical challenge during earthquake events. This latter limit is completely avoided with passive strategies which rely on localized devices that leverage a combination of deformability, strength, and energy absorption due to their localized inelastic damage [11, 2]. Passive protection is based on converting the system's input energy into both kinetic and strain potential energy which must be either absorbed, e.g. hysteretic elements [4, 7, 1, 3, 17, 18], or dissipated through heat, such as in viscous dampers [4, 15, 16, 10]. Semi-active devices represent a compromise between active and passive techniques [6, 23]. Similarly to active ones, the available semi-active control strategies are differentiated from what the sensors are demanded to monitor. Therefore, they are referred to as feedback, feed-forward, or feedback-feed-forward if the sensors monitor the response of the system, the excitation of the input, or both, respectively. In detail, a semi-active device is similar to a passive one with the added capability of varying its mechanical dynamical properties, i.e. damping coefficient and/or stiffness [24, 25]. This requires a low energy supply, e.g. battery pack, surpassing the active devices' main limitation. Throughout a control loop, the required varying action may be computed almost in real-time, i.e. with a minimum time lag. In the current study, the authors focused on semi-active control strategies for a single degree of freedom (SDOF) system employing a variable orifice damper (VOD). The current document is organized as follows. In section 2, a brief theoretical background on variable orifice dampers on a SDOF system is argued. In 3 the authors analyzed a SDOF VOD controlled case study under ideal conditions, whereas a VOD realistic model is finally discussed in sections 4 and 5.

2 VARIABLE ORIFICE DAMPERS ON A SDOF SYSTEM

Fluid viscous dampers consist of a piston demanded to convert seismic input energy into heat, typically filled with a compound of silicone oil with kinematic viscosity equal to 100 mm^2/s and specific weight equal to 9.78 kN/m^3. The fluid is non-toxic, inert, non-flammable, modellable as an uncompressible fluid, remaining stable for very long periods [24]. Specifically, a VOD device is a semi-active control technology that provides an adaptable damping force $f_d(t)$ by varying the size of the orifice of a viscous damper system according to the response recorded by the structure [9, 24]. Therefore, the motion equation of a lumped mass m SDOF structure base-excited with ground motion acceleration $\ddot{z}_g$ and equipped with a VOD is [9, 26]:

$$m\ddot{z}_1 + c\dot{z}_1 + kz_1 = -m\ddot{z}_g + f_d(t) \tag{1}$$

in which k is the stiffness, c is the damping coefficient, z_1 is the horizontal displacement of the SDOF mass. The semi-active dashpot damping force $f_d\,(t)$ depends on the system's relative velocity, i.e. the velocity of the piston rod:

$$f_d\,(t) = c_d\,(t)\,|\dot{z}_1\,(t)|^{\alpha}\,\mathrm{sgn}(\dot{z}_1(t)) \tag{2}$$

in which $c_d(t)$ is the regulated damping coefficient, which varies within a bounded range $[c_{d,\min};\, c_{d,\max}] = [1000; 10000]$Ns/m corresponding respectively to the fully open and completely

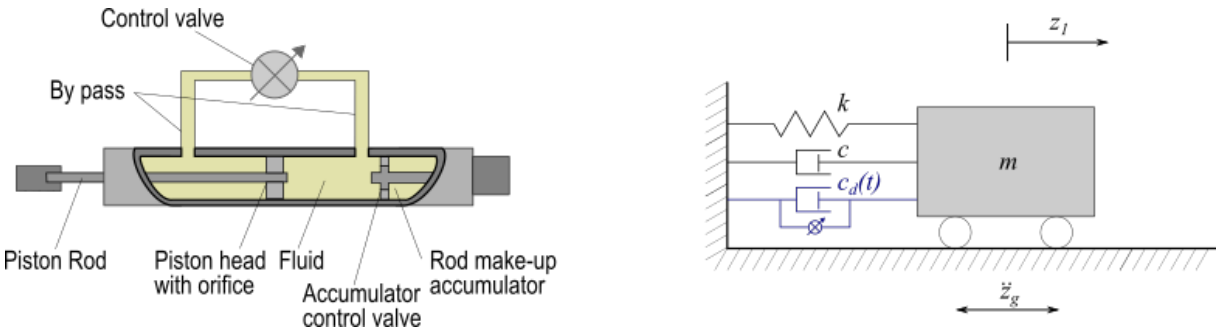

Figure 1: Broken out section view of a VOD and SDOF mechanical idealization model equipped with a semi-active fluid viscous VOD.

close valve conditions. α is a coefficient depending on the geometric size and design of the orifice and the piston, whose physically realizable values range from 0.1 to 2.0, experimentally determined with laboratory tests. In seismic applications it is desirable that α assume the smallest values, thus normally it spans between 0.1 to 1.0 [9]. In the present study, α was set to 0.1, a realistic common value. As shown in Fig.1, the presence of an accumulator and a control valve prevents any unwanted restoring force due to fluid compressibility. Typically, piston movements are characterized by a frequency lower than 4 Hz, without affecting the stiffness of the system. The dampers are often referred to as "inertial dampers" because of the dependence of the force output of the device on the speed of the fluid through the orifices. In Fig.1 the modifications needed to create a semi-active device are visible, in particular the addition of an external by pass loop with a control valve. In this form, the device is referred to as a "two-stage damper", because typically the control valve can only be in the "fully open" or in the "fully closed" position. The control valve is a direct current (DC) solenoid valve in which the solenoid coil can either be fully energized or de-energized [24]. A fundamental parameter of a semi-active fluid damper is the response time, which is the time needed for a complete variation of the damping coefficient, from minimum to maximum or vice versa. Therefore, there is a delay from the ideal behavior because the variation is not instantaneous. The response time is evaluated during the saturation condition of the command signal, and it can be separated into two different contributions. The first is a static response time t_1 related to the electronic response delay of the integrated electronic control unit (ECU) jointly with the presence of static friction, whereas the second one t_2 accounts for the time needed from the initial motion of the spool to the final position of the control valve, so the actual time in which the damping coefficient varies [24]. Depending on the structure of the valve in the application, the response time may or may not be identical for the opening procedure and the closing one, both for reasons related to the flow of oil inside the cylinder and for the presence of a reset spring. In general, this kind of delay is quite reduced and allows proper control of the device during the whole period. The specific value depends on the particular dimension of the valve and the damper used in the application, but in general the sum of t_1 and t_2 is safely in the range $20 \div 35$ ms.

3 UNCONTROLLED MODEL AND IDEAL CONTROL STRATEGIES

In the current study, the authors considered a numerical SDOF case study characterized by $m = 10000$kg, $k = 2000000$N/m, and $c = 2815$Ns/m, with a fundamental period of $T_1 = 0.4443$s ($f_1 = 14.1421$Hz). The Eq.1 may be rewritten using state-space formulation by setting the state vector $\boldsymbol{x} = [z_1, \dot{z}_1]^T$, the vector of measured observations $\boldsymbol{y} = [z_1, \dot{z}_1, \ddot{z}_1]^T$, and the

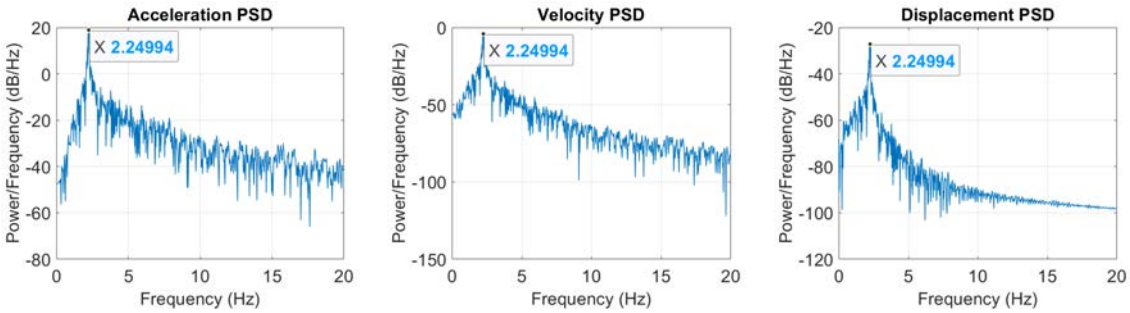

Figure 2: Spectral analysis of the uncontrolled SDOF system.

input vector $\boldsymbol{u} = [\ddot{z}_g, f_d(t)]^T$:

$$\dot{\boldsymbol{x}} = \boldsymbol{A}\boldsymbol{x} + \boldsymbol{B}\boldsymbol{u} \tag{3}$$

$$\boldsymbol{y} = \boldsymbol{C}\boldsymbol{x} + \boldsymbol{D}\boldsymbol{u} \tag{4}$$

being Eq.(3) named state equation and Eq.(4) named observation equation, with $\boldsymbol{A}$ the state matrix, $\boldsymbol{B}$ the input influence matrix, $\boldsymbol{C}$ the output influence matrix and $\boldsymbol{D}$ the direct transmission matrix [19]. These matrices are defined as follows:

$$\boldsymbol{A} = \begin{bmatrix} 0 & 1 \\ -\frac{k}{m} & -\frac{c}{m} \end{bmatrix}; \boldsymbol{B} = \begin{bmatrix} 0 & 0 \\ -1 & \frac{1}{m} \end{bmatrix}; \boldsymbol{C} = \begin{bmatrix} 1 & 0 \\ 0 & 1 \\ -\frac{k}{m} & -\frac{c}{m} \end{bmatrix}; \boldsymbol{D} = \begin{bmatrix} 0 & 0 \\ 0 & 0 \\ -1 & \frac{1}{m} \end{bmatrix} \tag{5}$$

Eqs.(3)-(4)-(5) describe a state space model with two inputs, i.e. the earthquake loading $m\ddot{z}_g$, in this study referred to 1940 El Centro earthquake, and the nonlinear damping force $f_d(t)$. Therefore, six transfer functions are related respectively to displacement, velocity, and acceleration given by the first seismic input, whereas the latter three are related to the VOD damping force. Foremost, the authors implemented in Matlab Simulink [8] an initial uncontrolled model for a reference behavior before adding the VOD system, obtaining displacement, velocity, and acceleration of the SDOF system only. Spectral analysis of the three output signals was performed to provide further deeper insights, as illustrated in Fig.2. The authors performed a trial-and-error approach based on the power spectral density (PSD) of the signals in order to determine the optimal sampling time. A noteworthy aspect evidenced from the PSD graphs for the specific SDOF structure equipped with a VOD ideally controlled is the resonance frequency peak located around 3Hz. Thereafter, the authors implemented a model including the VOD system acting as a passive damper, i.e. without any control. As illustrated in Fig.3, a feedback loop monitors the velocity value to evaluate the damping force according to Eq.(2), in which c_d is constant in time. Using an initial sinusoidal input calibrated at the resonance frequency of the SDOF, the authors validated the effectiveness of the implementation and the hysteresis loops, thus simulating an ideal laboratory test of the device.

Afterward, the authors implemented two ideal control algorithms with saturation (since adaptive damping varies within a bounded range), neglecting, for the moment, the time delay in the VOD adaptive response, i.e. the proportional-integrative-derivative (PID) control algorithm, and the model predictive control (MPC) algorithm [12]. The PID controller regulates the gain parameters of the proportional, derivative, and integrative blocks relying on the error between the actual value and a reference value of a control variable [25], i.e. in this case the system's velocity as depicted in 4 (a). It has been tuned with the built-in PID tuner app inside the Simulink

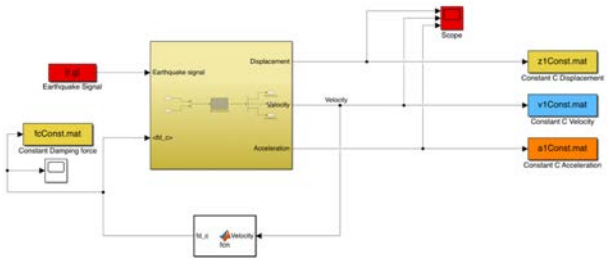

Figure 3: Matlab Simulink model of the SDOF structure under study equipped with a viscous VOD device without any control system, thus acting as a passive device.

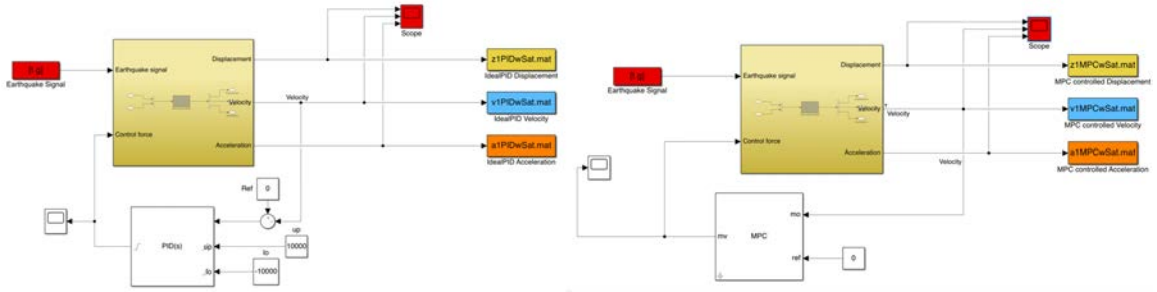

(a) (b)

Figure 4: Ideal control strategies with upper and lower saturation constraints: (a) PID controller, (b) MPC controller.

environment, through the linearization of the plant represented by the state space model of the structure. The tuning procedure of the controller was carried out by choosing values that represented a compromise between robust behavior and quick response time. On the other hand, the MPC controller leverages a built-in Kalman filtering action which observes the velocity output from the state-space model aiming to stabilize the structure as quickly as possible toward a nil reference velocity value [25]. In this specific MPC controller, based on the PSD analyses of the uncontrolled system, the sampling time was set equal to 1/100 seconds and one millisecond, and the prediction and control horizons were set to 100 units of sampling time. The PID does not virtually require a detailed model of the dynamical system, whereas, on the contrary, MPC is based on a linearization of the specific state-space model since it builds a predictive model of future states based on the history of the input/output relation of the transfer functions [25]. The results of simulations conducted under El Centro earthquake loading are reported in Fig.5. The displacement, velocity, and acceleration signals with the ideal PID and MPC algorithm present the desirable controlled behavior. The PID and MPC control algorithms guaranteed a lower acceleration of the SDOF system, thus with a more stable behavior throughout the whole simulation. These graphs show that an ideal control force is capable of effectively reducing the values of acceleration of the SDOF structure, and consequently also the velocity and displacement responses. In Fig.6, the authors reported some bar graphs illustrating the peak values of each signal among the different control strategies. It is evident that the MPC algorithm succeeded to forecast the dynamics of the system, consequently delivering a better-controlled behavior with lower velocity and acceleration peaks. On the other hand, the PID controller maintains the signals within a certain threshold, however, it seems not capable to

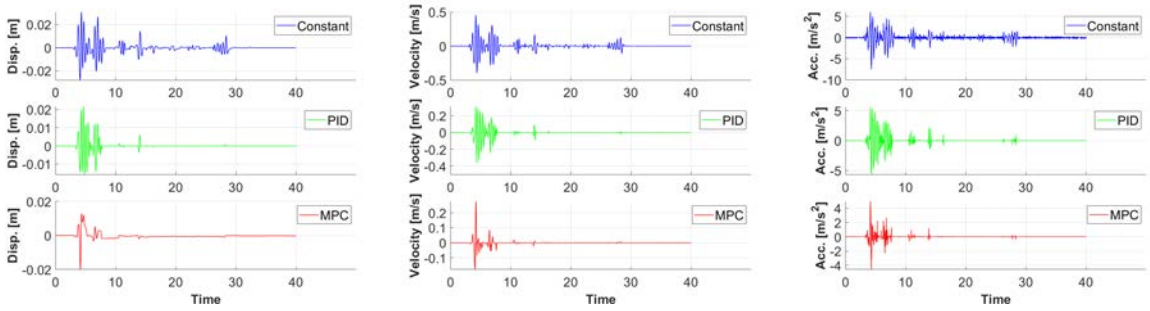

Figure 5: Displacement, velocity and acceleration of SDOF under 1940 El Centro earthquake loading with passive damper (blue), ideal PID (green), and ideal MPC control (red).

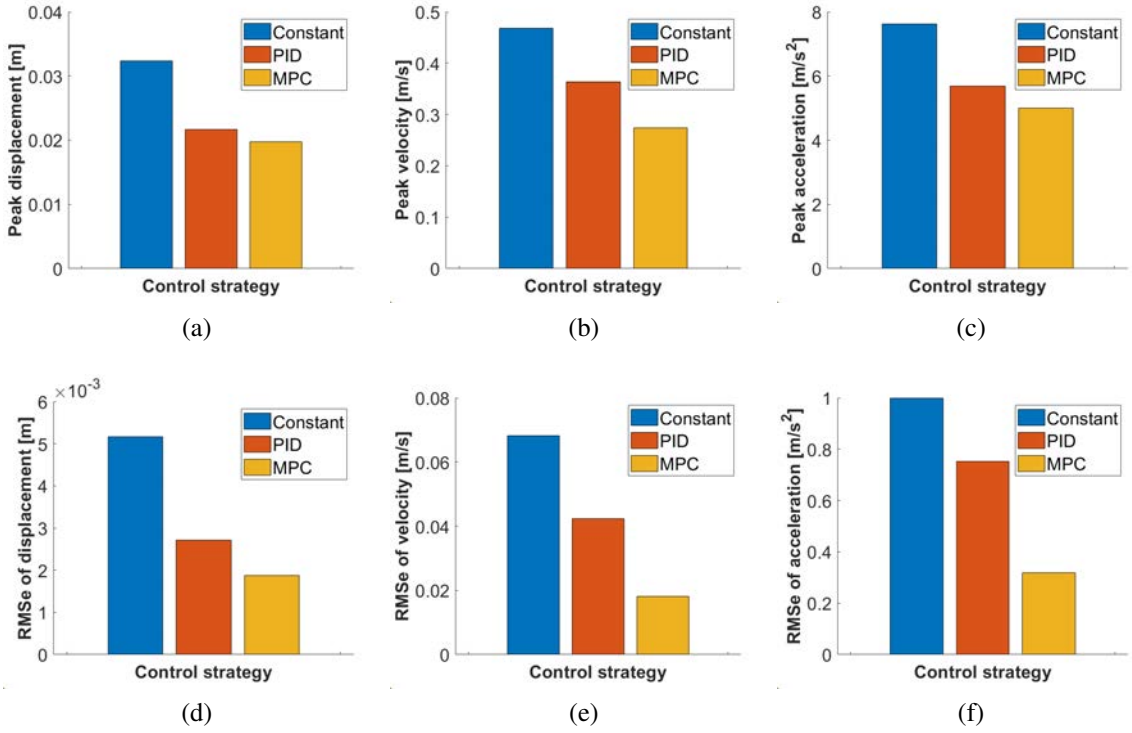

Figure 6: Peak and RMSe values of displacement (top left), velocity (top right), and acceleration (bottom) in constant case (blue) ideal PID case (orange) and ideal MPC case (yellow).

reduce the acceleration and velocity of the same magnitude of MPC. The graphs also illustrate the signals' root mean square error (RMSe) among the various control strategies. Once again, MPC provides noticeable performances with respect to the other control algorithms.

The authors considered these ideally controlled results as a reference condition for the next more realistic simulations. In the next section, the authors modelled the VOD according to its real mathematical model, i.e. even considering a certain time delay in the VOD response.

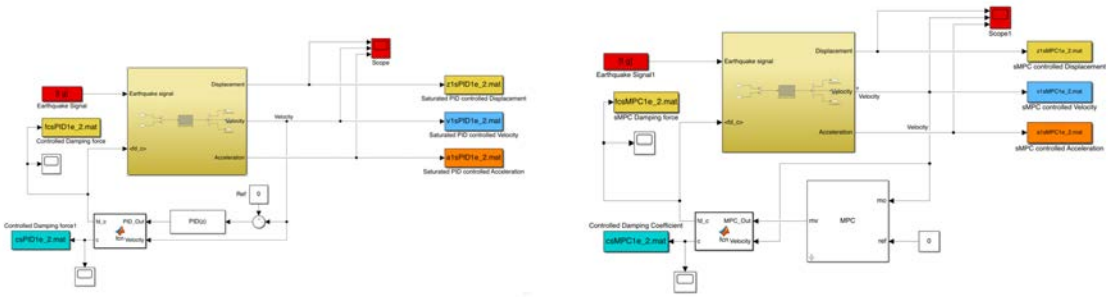

(a) (b)

Figure 7: Simulink realistic models with a sampling time of 0.01s: (a) PID controller; (b) MPC controller.

4 REALISTIC OPTIMALLY CONTROLLED MODEL

In this section, the authors first analyzed a realistic controlled SDOF system without any time delay based on the reference results provided by the ideal PID and MPC algorithms in the previous section. According to the PSD analysis of the uncontrolled system, the authors determined the minimum sampling time of the velocity signal with a trial-and-error procedure. Indeed, this is a critical parameter that is fed to the controller block for computing the required control damping force. Specifically, in Fig.2 the diagrams were graphically limited up to 20Hz, however, the analyses were computed up to 500 Hz. The PSD assumes a value of -100 dB at 50 Hz, therefore an ideal cut-off over 50Hz can be set due to their low power. Therefore, according to the Shannon-Nyquist theorem, the minimum sampling frequency was chosen equal to 100Hz in the simulations. Furthermore, a sampling frequency of 1000Hz was even employed to check the effects of a different sampling time on the control algorithm performances. The authors have chosen these two different sampling frequencies to preliminary evaluate the possibility of implementing the analyzed control algorithms in a real-world application, based on the nowadays microcontrollers available in the market with sufficient computing power.

The authors adopted a specific strategy in order to build a model based on an optimal control algorithm and also consider the real behavior of the VOD device. The ideal controller of the previous section was used as a reference for the maximum possible value of the control force to the system $f_d^{(\text{ref})}$. Therefore, a new function computed the value of the damping coefficient of the device needed to obtain the control force input by the controller using the inverse formula of Eq.2:

$$c_d\left(t\right) = \frac{f_d^{(\text{ref})}\left(t\right)}{\left|\dot{z}_1\left(t\right)\right|^{\alpha} sgn(\dot{z}_1)} \tag{6}$$

It is worth reminding that when the value of the variable damping coefficient $c_d\left(t\right)$ from Eq6 falls outside the admissible range of the device $[c_{d,\min}; c_{d,\max}]$ the damping coefficient saturates at the maximum or minimum limit of the range.

Fig.7 (a) shows the model built with the PID controller with a velocity sampling frequency of 100 Hz. The implemented Matlab function of Eq.6 is fed with two inputs, i.e. the ideal maximum control force from the PID controller $f_d^{(\text{ref})}$ and the velocity value retrieved from the state space equation. This creates a feedback loop modeling of the semi-active fluid VOD system. For the sake of comparisons of the effectiveness of the results, the same model was

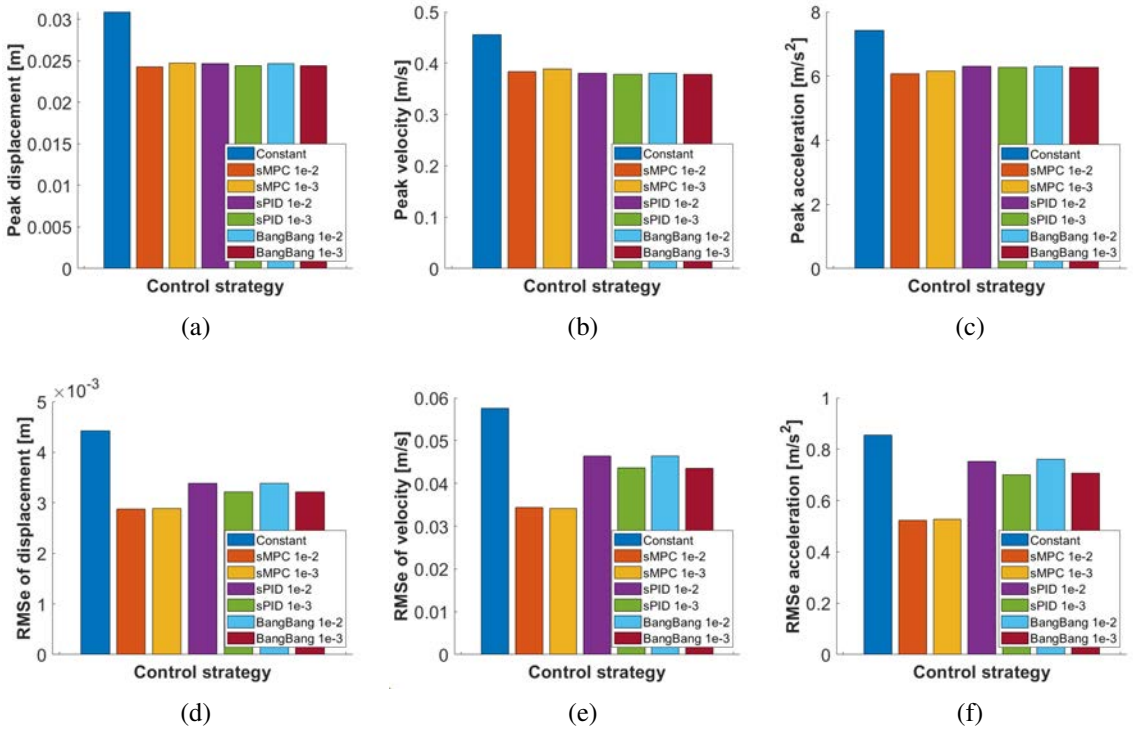

Figure 8: Peak and RMSe values of displacement (top left), velocity (top right), and acceleration (bottom) in constant case (blue), realistic MPC with sampling time 1e-2 (orange), realistic MPC with sampling time 1e-3 (yellow), realistic saturated PID with sampling time 1e-2 (purple), saturated PID with sampling time 1e-3 (green), BangBang with sampling time 1e-2 (light blue), and BangBang with sampling time 1e-3 (dark red).

realized with a different sampling time equal to one millisecond. Moreover, a further variation of this model was implemented considering the case in which the damper works in a two-stage condition (*BangBang strategy*). In this latter case, the damping coefficient can only assume the limit admissible values, i.e. saturating at the higher or the lower limits, viz. when the computed damping coefficient is above or below a certain threshold. The authors implemented this third BangBang condition reflecting that many semi-active fluid viscous dampers in real-world applications operate in those two-stage conditions. A third Simulink model, see Fig.7 (b), with the same architecture was implemented using the MPC control algorithm, with two different sampling frequencies of 100 Hz and 1000 Hz for further comparisons. Once again, the input from the controller enters a function block that computes the ideal damping coefficient needed to obtain the control force desired from the controller $f_d^{(\mathrm{ref})}$. Thereafter, a function block outputs the variable damping coefficient of the device, providing the real control force considering the physical limitations of the actual VOD system. These three analyzed models may represent an almost physically accurate behavior of the semi-active fluid VOD although some crucial modeling aspects are still neglected at this level, i.e. the time delay in the damping coefficient variation or the various noise sources, e.g. in the velocity measures.

Similarly to before, the performance results were inspected through the bar graphs concerning the peak values and the RMSe values of the output signals. In Fig.8 the passive constant damper case is depicted in blue, followed by the two MPC simulations with progressively in-

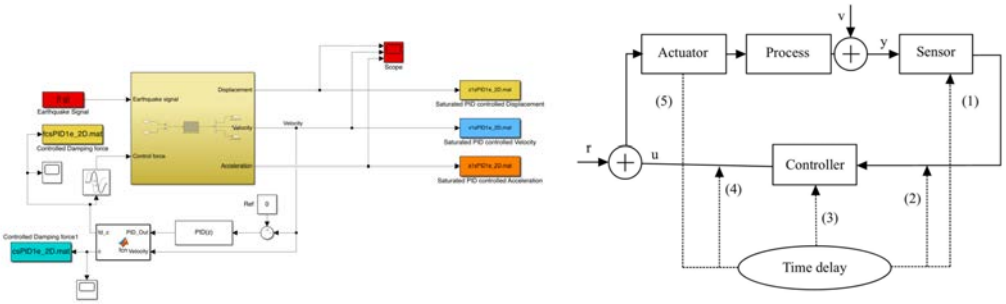

(a) (b)

Figure 9: (a) Simulink model implementing the delay of the real semi-active fluid viscous damper; (b) generic control system and possible sources of delay.

creasing sampling frequency, and finally followed by the four PID simulations, the first two with the variable damping coefficient within $[c_{d,\min}; c_{d,\max}]$, and the latter two with the two-stage BangBang strategy. At first sight, it is evident that any control strategy produced improved behaviors compared to the passive constant damper only. The graphs demonstrated that the different sampling times do not affect the peak values of the various different control algorithms. Moreover, it is noteworthy that the results of the variable damping PID simulation and the two-stage BangBang performed very similarly to each other. This means that the BangBang strategy works as well as the standard PID one in order to reduce the peak values, despite being much easier to implement. The RMSe values show that the MPC algorithm still performs better than a standard PID control algorithm, with a decrease of approximately 15% in all signals. Furthermore, the BangBang algorithm presents the same performances as the standard PID, but with cheaper installation costs and requires less computational effort.

5 TIME DELAY ISSUE MODELING

The previous simulations demonstrated the effectiveness of the PID and MPC control algorithms to improve the dynamic behavior of the SDOF system reducing the peak values and RMSe of the signals. Nevertheless, the implemented model hitherto neglected the real delay of the physical device to activate the required response. Specifically, as depicted in Fig.1, the semi-active fluid viscous VOD damper implements a solenoid control valve in the outside by pass loop. This control valve requires a certain amount of time to change its position from completely open to closed states with an average delay of $20 \div 35$ms [24]. Therefore, in the current section, the authors implemented a controlled SDOF model considering a conservative constant delay of 30ms as depicted in Fig.9.

The performances of the various control algorithm considering time delay were compared by evaluating peak values and RMSe of displacement, velocity, and acceleration signals, as shown in Fig.10. In all the control strategies, the peak values were still reduced with respect to the passive damper. Moreover, the performances present still improvements with respect to the uncontrolled system, notwithstanding that the presence of any delay usually becomes a critical issue jeopardizing the effectiveness of the control algorithms. This may be related to a proper tuning of the control system which does not require a strongly impulsive behavior of the semi-active device. On the other hand, focusing on the RMSe, the control systems with delay present a significant variation with respect to Fig.8. In general, the MPC exhibits lower

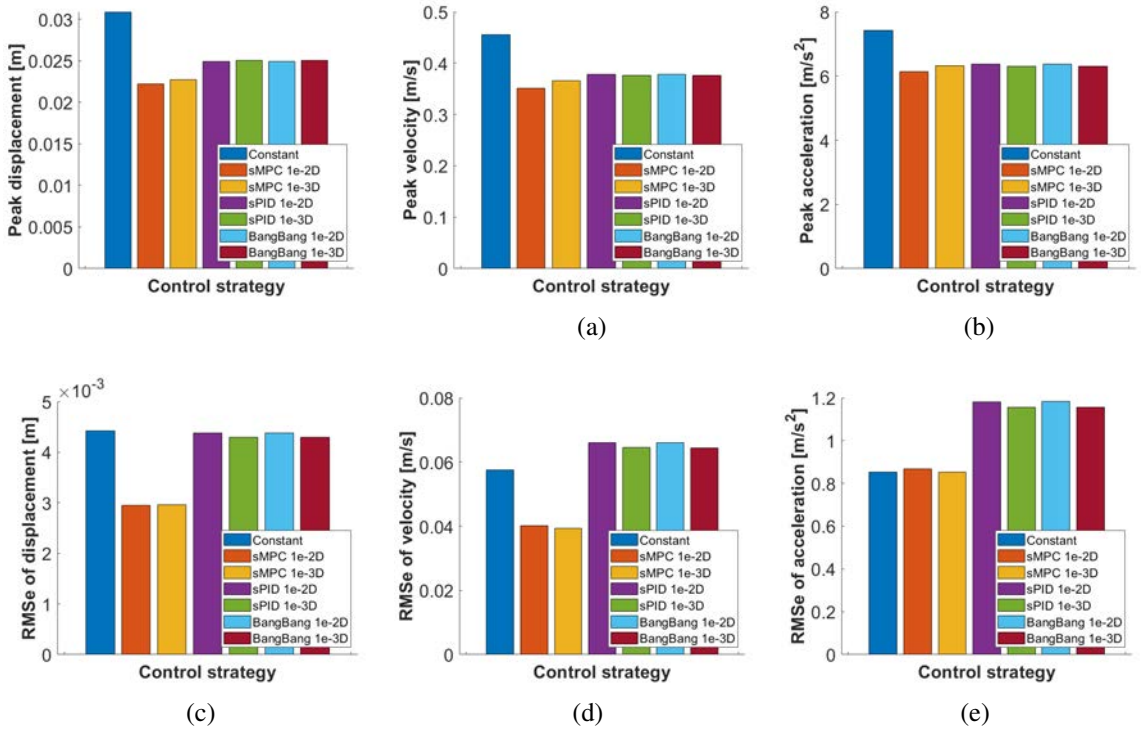

Figure 10: Peak and RMSe values of displacement (top left), velocity (top right), and acceleration (bottom) considering the delay of the sinusoidal valve of the semi-active fluid viscous damper in constant case (blue), MPC with sampling time 1e-2 (orange), MPC with sampling time 1e-3 (yellow), saturated PID with sampling time 1e-2 (purple), saturated PID with sampling time 1e-3 (green), BangBang with sampling time 1e-2 (light blue), and BangBang with sampling time 1e-3 (dark red).

values of RMSe concerning the other methods in virtually all cases, except for the acceleration signal which delivers RMSe of the same order of magnitude as the passive device. However, in contrast with Fig.8, in the current delay case of Fig.10, the RMSe appears in general higher than the passive constant damper for the other control strategies. The MPC control algorithm performance level is strictly related to its capacity of modifying the response depending on the previous input-output monitored data. This is a prerogative feature of the MPC only and not of the PID controller. In conclusion, considering the delay, a certain amount of performance degradation in the control loop is visible, especially in the RMSe graphs. However, the authors highlight that the current simulations were performed with a constant 30ms of delay, i.e. a quite conservative condition very close to the worst-case scenario as described in [24]. Therefore, the current results may be still considered acceptable in the context of a possible real implementation of the semi-active device. In the control theory field, the delay in a system is a well-known problem, which can be classified as either loss problems or delay problems [20]. The acknowledged loss problems appear when the total delay of the system (computing time delay, the delayed response of the components, etc.) reaches a value greater or equal to the monitoring signals' sampling time. On the contrary, the delay issue manifests when the total delay of the system assumes a value smaller than the sampling time. Focusing on the current manuscript, the simulation of VOD delay has fallen into the category of loss problems, since the delay's

entity was higher than the chosen velocity sampling time. Nevertheless, a comprehensive study of the effects of a loss problem on a system is always challenging for different reasons, one of all the delay should be properly modeled as a random variable.

6 CONCLUSIONS

In this study, the authors analyzed a preliminary numerical application of a variable orifice damper equipped to a single degree of freedom structure. The authors focused on the vibration control of a SDOF system starting from an uncontrolled system modeled in Matlab Simulink under El Centro earthquake dynamic excitation. A simplified linearized state-space model was implemented to reduce the level of model complexity and computational weight. Thereafter, a VOD was deployed on the SDOF system but without any controller, i.e. acting as a passive constant damper device. Afterwards, the authors implemented a VOD with an ideal controller based on the PID and the MPC algorithms with two different velocity sampling frequencies (100Hz and 1kHz). The authors chosen these two different sampling frequencies to preliminary evaluate the possibility of implementing the analyzed control algorithms in a real-world application, based on the nowadays microcontrollers available in the market with sufficient computing power. The ideally controlled results were set as a reference for the subsequent improved models toward a more realistic control strategy. Specifically, the PID and MPC controllers provided a variable damping coefficient through a Matlab function with upper and lower saturation bounds. The widespread simplified PID with BangBang strategy was also considered. This latter strategy considers only two levels of damping coefficient in the device, corresponding i.e. to the fully open (minimum damping) and fully closed (maximum damping) valve states. The controlled output SDOF behavior generally highlighted a better performances of the MPC with respect to PID algorithm. However, MPC poses at each sampling instant an optimization problem, which must be solved with a fast numerical algorithm in a reliable way. The feasibility of the optimal solution may be robust to noise which may instead compromise the stability of the entire system. It is noteworthy that real-world implementations demands a trade-off between performance and complexity of the system, and for this reason, frequently the PID controller with a BangBang strategy is chosen over other solutions [25]. Eventually, the authors also implemented SDOF control strategies considering a common issue, i.e. the time delay problem caused from the reactiveness time required for the solenoid valve within the VOD by pass system passing from fully open to closed states and vice versa. Future research studies may involve more accurate modeling, e.g. accounting for measurement noise, extensions to MDOF systems and real-world applications feasibility with recent IoT devices and microprocessors, even integrating artificial intelligence methodologies.

7 ACKNOWLEDGMENTS

This research has been supported by the ADDOPTML project: “ADDitively Manufactured OPTi-mized Structures by means of Machine Learning” (No: 101007595) belonging to the Marie Skłodowska-Curie Actions (MSCA) Research and Innovation Staff Exchange (RISE) H2020-MSCA-RISE-2020. Their support is highly acknowledged.

REFERENCES

[1] Angelo Aloisio, Marco Martino Rosso, Asif Iqbal, and Massimo Fragiacomo. Hysteresis modeling of timber-based structural systems using a combined data and model-driven

approach. *Computers & Structures*, 269:106830, 2022.

[2] Gebrail Bekdaş, Sinan Melih Nigdeli, and Aylin Ece Kayabekir. Introduction and overview: Structural control and tuned mass dampers. In *Optimization of Tuned Mass Dampers*, pages 1–13. Springer, 2022.

[3] Eleonora Bruschi and Virginio Quaglini. Assessment of a novel hysteretic friction damper for the seismic retrofit of reinforced concrete frame structures. In *Structures*, volume 46, pages 793–811. Elsevier, 2022.

[4] Eleonora Bruschi, Virginio Quaglini, and Paolo M Calvi. A simplified design procedure for seismic upgrade of frame structures equipped with hysteretic dampers. *Engineering Structures*, 251:113504, 2022.

[5] Attilio Carotti. *Meccanica delle strutture e controllo: modellistica di edifici, ponti, camini, strutture speciali*. Springer Science & Business Media, 2001.

[6] Fabio Casciati, Jose Rodellar, and Umut Yildirim. Active and semi-active control of structures–theory and applications: A review of recent advances. *Journal of Intelligent Material Systems and Structures*, 23(11):1181–1195, 2012.

[7] Fabio Di Trapani, Marzia Malavisi, Giuseppe Carlo Marano, Antonio Pio Sberna, and Rita Greco. Optimal seismic retrofitting of reinforced concrete buildings by steel-jacketing using a genetic algorithm-based framework. *Engineering Structures*, 219:110864, 2020.

[8] Simulink Documentation. Simulation and model-based design, 2020.

[9] Hossein Ghaffarzadeh, Ebrahim Alizadeh Dehrod, and Nima Talebian. Semi-active fuzzy control for seismic response reduction of building frames using variable orifice dampers subjected to near-fault earthquakes. *Journal of Vibration and Control*, 19(13):1980–1998, 2013.

[10] Rita Greco, Jennifer Avakian, and Giuseppe Carlo Marano. A comparative study on parameter identification of fluid viscous dampers with different models. *Archive of Applied Mechanics*, 84:1117–1134, 2014.

[11] GWea Housner, Lawrence A Bergman, T Kf Caughey, Anastassios G Chassiakos, Richard O Claus, Sami F Masri, Robert E Skelton, TT Soong, BF Spencer, and James TP Yao. Structural control: past, present, and future. *Journal of engineering mechanics*, 123(9):897–971, 1997.

[12] Štefan Kozák. From pid to mpc: Control engineering methods development and applications. In *2016 cybernetics & informatics (K&I)*, pages 1–7. IEEE, 2016.

[13] Giuseppe C Marano, Marco M Rosso, and J Melchiorre. Optimization as a tool for seismic protection of structures. In *Seismic Isolation, Energy Dissipation and Active Vibration Control of Structures: 17th World Conference on Seismic Isolation (17WCSI)*, pages 100–113. Springer, 2023.

[14] Giuseppe Carlo Marano and Giuseppe Quaranta. A new possibilistic reliability index definition. *Acta mechanica*, 210(3-4):291–303, 2010.

[15] Giuseppe Carlo Marano, Francesco Trentadue, and Rita Greco. Stochastic optimum design criterion of added viscous dampers for buildings seismic protection. *Structural Engineering and Mechanics, An Int'l Journal*, 25(1):21–37, 2007.

[16] C Pettorruso, E Bruschi, V Quaglini, et al. Supplemental energy dissipation with prestressed lead extrusion dampers (p-led): Experiments and modeling. In *COMPDYN 2021 8th ECCOMAS Thematic Conference on Computational Methods in Structural Dynamics and Earthquake Engineering*, pages 1–14, 2021.

[17] Virginio Quaglini, Carlo Pettorruso, and Eleonora Bruschi. Design and experimental assessment of a prestressed lead damper with straight shaft for seismic protection of structures. *Geosciences*, 12(5):182, 2022.

[18] Virginio Quaglini, Carlo Pettorruso, Eleonora Bruschi, et al. Experimental and numerical assessment of prestressed lead extrusion dampers. *INGEGNERIA SISMICA*, 38(2):46–69, 2021.

[19] Carlo Rainieri. *Operational Modal Analysis for seismic protection of structures*. PhD thesis, 2008.

[20] Kang G Shin and Xianzhong Cui. Computing time delay and its effects on real-time control systems. *IEEE Transactions on control systems technology*, 3(2):218–224, 1995.

[21] Tsu T Soong and Michalakis C Costantinou. *Passive and active structural vibration control in civil engineering*, volume 345. Springer, 2014.

[22] TT Soong. State-of-the-art review: active structural control in civil engineering. *Engineering Structures*, 10(2):74–84, 1988.

[23] T.T. Soong and Billie Spencer. Active, semi-active and hybrid control of structures. *Bulletin of the New Zealand Society for Earthquake Engineering*, 33:387–402, 09 2000.

[24] M.D. Symans and M.C. Constantinou. *Technical Report NCEER-95-0011 - Development and Experimental Study of Semi-Active Fluid Damping Devices for Seismic Protection of Structures*. National Center For Earthquake Engineering Research, 1995.

[25] Andrea Troise. Modelling and control of semi-active fluid viscous dampers in structural vibration optimization, 2022.

[26] N Wongprasert and MD Symans. Experimental evaluation of adaptive elastomeric base-isolated structures using variable-orifice fluid dampers. *Journal of Structural Engineering*, 131(6):867–877, 2005.